AT-GIS: Highly Parallel Spatial Query Processing with Associative Transducers

Peter Ogden
Imperial College London
p.ogden12@imperial.ac.uk

David Thomas
Imperial College London
d.thomas1@imperial.ac.uk

Peter Pietzuch
Imperial College London
prp@imperial.ac.uk

ABSTRACT

Users in many domains, including urban planning, transportation, and environmental science want to execute analytical queries over continuously updated spatial datasets. Current solutions for large-scale spatial query processing either rely on extensions to RDBMS, which entails expensive loading and indexing phases when the data changes, or distributed map/reduce frameworks, running on resource-hungry compute clusters. Both solutions struggle with the sequential bottleneck of parsing complex, hierarchical spatial data formats, which frequently dominates query execution time. Our goal is to fully exploit the parallelism offered by modern multi-core CPUs for parsing and query execution, thus providing the performance of a cluster with the resources of a single machine.

We describe AT-GIS, a highly-parallel spatial query processing system that scales linearly to a large number of CPU cores. AT-GIS integrates the parsing and querying of spatial data using a new computational abstraction called *associative transducers* (ATs). ATs can form a single data-parallel pipeline for computation without requiring the spatial input data to be split into logically independent blocks. Using ATs, AT-GIS can execute, in parallel, spatial query operators on the raw input data in multiple formats, without any pre-processing. On a single 64-core machine, AT-GIS provides 3× the performance of an 8-node Hadoop cluster with 192 cores for containment queries, and 10× for aggregation queries.

1. INTRODUCTION

Sources of spatial data are growing at an ever increasing rate. Crowd-sourced projects such as OpenStreetMap [21] create continuously-updated, planetary-scale datasets with 100s of millions of objects—the latest weekly OpenStreetMap snapshot is over 40 GBs compressed, 596 GBs uncompressed. High-resolution imaging, from microscopes to satellites, is another source of massive spatial data that can be analysed. In urban planning [5], transportation [52], environmental science [22] and medical image analysis [31], data scientists therefore face the task of executing spatial analytics queries over large datasets in an efficient manner. Spatial queries include selecting shapes within regions, summarising shapes that meet given criteria, and finding all intersecting or overlapping shapes. From these primitives, more complex queries for testing for shape similarity between datasets or determining changes over time can be built.

In domains with new or constantly updated spatial datasets, a key requirement is a low *data-to-query* time [2], i.e. the time to obtain a query result after the data becomes available. In pathology image analysis, in which segmented image data is queried for anomalous artefacts, it is one of the limiting factors for fast diagnosis [60]; for the OpenStreetMap dataset, this value determines how quickly new geographic features can be incorporated into any analysis.

Currently users who query large spatial datasets must either use relational database management systems (RDBMS) with spatial indexing support, such as *PostGIS* [25] or *Oracle Spatial* [45], or employ a distributed compute framework on a cluster, such as *Hadoop-GIS* [1] or *SpatialHadoop* [13]. Both approaches, however, suffer from a slow data-loading phase, which must occur before spatial queries can be run. RDBMS can only offer fast spatial query processing after the data has been fully parsed, loaded and indexed—in our experiments, loading the complete OpenStreetMap dataset into PostGIS takes over 90 minutes, with an additional 75 minutes to construct the index. Conversely, distributed frameworks with indexing support can offer good query performance, but they require substantially more computational resources than single machine deployments. To spread the load between cluster nodes, they must partition the spatial datasets, e.g. by loading it first into a distributed file system, increasing the total data-to-query time [34].

To reduce the data-to-query time for large spatial datasets, it is paramount to exploit parallelism when parsing, indexing and querying the data. If the original dataset format is simple, as it is the case for the *well-known text* (WKT) and *well-known binary* (WKB) spatial formats [42], data-parallelism can be gained from partitioning the input data into independent, fixed-sized blocks and processing them separately [58]—parsing and some spatial filtering can then be performed in parallel, while aggregation and join queries require the combination of all of the data. Unfortunately this simple partitioning approach does not work for more complex, though widely used spatial data formats, including GeoJSON [19] and XML [43]. Due to their hierarchical nature, these formats make it difficult to determine at which boundaries to split the data into independent parts without resynchronising the parser [46].

Our goal is to design a single-machine system for spatial query processing over large datasets that fully exploits the parallelism of modern multi-core CPUs. To minimise data-to-query time, our system should ingest commonly-used source data formats without any pre-processing, following the *NoDB* philosophy of executing queries over raw data [2]. The main challenge is that such a system must parallelise the parsing, indexing and spatial query execution. To scale to many CPU cores, it must thus minimise any inter-thread communication or access to global state. While the NoDB philosophy may result in increased I/O bandwidth when the input

SIGMOD'16, June 26-July 01, 2016, San Francisco, CA, USA

 ISBN 978-1-4503-3531-7/16/06…$15.00

DOI: http://dx.doi.org/10.1145/2882903.2882962

data format is complex or queries require multiple data passes, this can be mitigated through on-the-fly indexing and temporary storage.

We describe the design and implementation of **AT-GIS**, a system for highly-parallel spatial query processing on multi-core CPUs that operates on raw spatial datasets. For containment and aggregation queries, AT-GIS constructs a parallel processing pipeline that parses the data and executes the query in a single pass with constant memory. For spatial join queries, AT-GIS employs two passes, separating parsing and partitioning from the join computation.

To achieve parallelism across many CPU cores, AT-GIS uses a new computational model called **associative transducers (ATs)**. ATs allow for the data-parallel execution of otherwise sequential operations, making them a natural model for the processing of complex spatial data formats. With ATs, it is possible to separate parsing, extraction and spatial operator execution into distinct transducers that can be pipelined together. Instead of allocating a thread per transducer, which would limit the degree of parallelism and require synchronisation between them, in ATs each thread executes the entire pipeline, for separate blocks of the input data. Intermediate results in the pipeline are kept local to each thread, with only the final result synchronised and shared globally.

ATs have two features that enable them to execute multiple dependent spatial query processing stages in a data-parallel fashion: (i) they perform some degree of *speculation* during execution; and (ii) they leverage the *associativity* of spatial query operations. Parsing, data extraction and spatial operations are performed using finite and pushdown state machines, modified to support out-of-order operation through efficient speculative execution from all possible starting states. A formal model based on transducers allows multiple ATs to be pipelined while maintaining associativity. This permits AT-GIS to implement complex spatial operators using associative algorithms so that partial results can be merged.

We show experimentally that AT-GIS operates efficiently on multiple data formats: it performs spatial aggregation queries on GeoJSON or WKT-formatted OpenStreetMap data 2× faster than SpatialHadoop on the same hardware, despite not using an index; it is 10× faster than an 8-node Hadoop-GIS cluster, which has 3× the CPU cores and already pre-partitioned data. For spatial join queries, the time that AT-GIS requires to read and partition the dataset in parallel is less than 20% of the time taken to execute the join, with the total query time comparable to that of a larger cluster-based system. AT-GIS also achieves similar query performance, but with a much lower data-to-query time, as a commercial parallel DBMS with indexing for containment and aggregation queries and shows a two orders-of-magitude improvement over PostGIS.

The rest of paper is structured as follows: §2 discusses the problem and existing solutions for spatial query processing over large datasets; §3 describes the model of associative transducers for spatial queries; §4 presents the design of AT-GIS, explaining its query processing stages; §5 evaluates our prototype implementation; §6 discusses related work; and §7 concludes.

2. SPATIAL QUERY PROCESSING

We now introduce spatial queries (§2.1) and the challenges when querying large datasets (§2.2). We then discuss two approaches for large-scale spatial query processing (§2.3): spatial extensions to RDBMS and distributed systems based on the map/reduce model.

2.1 Spatial queries

As the size of data has increased, so has data that incorporates a spatial component [33]. Given that spatial searching is widely used in modern web applications [12], a common use of spatial data is in relating places on the surface of the earth. Other uses for geospatial processing are finding correlations between datasets acquired from different sources—a key component of current geospatial datastore benchmarks [16, 51]. As well as geospatial data, there is a growing use of spatial analytics in medical imaging, in particular pathology, in order to automate the process of finding a diagnosis from high-resolution digital microscopy images [31].

Listing 1: Example fragment of GeoJSON file

```
{ "type": "FeatureCollection",
  "features": [
    { "type": "Feature",
      "geometry": {
        "type": "GeometryCollection",
        "geometries": [
          { "type": "GeometryCollection",
            "geometries": [/* Shape Data */]},
          { "type": "LineString",
            "coordinates": [[1.1, 0.0],[1.2, 1.0]]}
        ]}
      "id": 1234,
      "properties": { /* User Data */ }
    }
  ]
}
```

In this paper, we consider spatial datasets as collections of *objects*. Each object consists of a *geometry*, as defined by the Open Geospatial Consortium Standard [42], and associated *metadata*. Supported types of geometries are linestrings, polygons, multipolygons and collections. An example of a dataset consisting of one object is given in Listing 1. Here the geometry is a collection, and the metadata is both an identifier and user-provided properties.

We focus is on three classes of spatial queries:

Containment queries are the most basic primitive in spatial processing and perform a filtering operation on the data. The canonical example is finding all geometries contained within a region, but any filtering query against a defined set of reference objects can be considered as containment.

Aggregation queries are an extension of containment queries and involve some summarisation over the filtered result set. The summary can be numeric, such as the average area of all selected geometries, or spatial, e.g. computing the set-spatial union of all shapes in the set. Multiple aggregations can also be performed simultaneously, as done by `GROUP BY` SQL statements.

Join queries are one of the most expensive operations associated with spatial querying because, in the worst case, every geometry in one dataset must be compared with every geometry in another. To reduce the number of pairs of geometries for comparison and to parallelise the computation, it is common to divide the shapes into *spatial partitions* [48, 24]. Each partition contains a subset of the dataset within some defined area, and disjoint partitions can thus be processed in parallel. Partitioning allows join processing to scale to multiple CPU cores, but introduces an additional partitioning step.

2.2 Scalability challenges

The wide availability of always-connected, location-aware mobile devices is causing a massive growth in the quantity of spatial data being generated and stored [63, 61]. Crowd-sourced mapping and behavioural data has become mainstream for uses such as navigation [21] and epidemiology [23], with the number of users continuing to grow. Standards are already being developed to support the next generation of sensor and IoT systems in which updates will be continuously streamed [7], thus requiring spatial data processing systems to operate without prior offline data partitioning.

Since CPU clock speeds have remained relatively constant, multi-core processing is essential for achieving fast query results [57]. For a low *data-to-query* time, all query processing stages must be parallelised. Most data querying systems now implement some form of parallelism once the data is loaded; few systems, however,

consider how data can be loaded in parallel. Loading data in parallel requires the concurrent execution of two operations: *parsing* the source data format and *partitioning* or *indexing*. When the data on disk is not spatially partitioned, distributing the parsing in cluster systems causes significant I/O load as geometries are shuffled from the node responsible for parsing to the nodes with the correct spatial partitions [47]. The same is true when loading data in parallel into a single-node sharded database: here network I/O is replaced by disk I/O when moving geometries to the correct database instance.

Following a NoDB philosophy [2], a scalable spatial querying system should support the input data efficiently no matter what its format is. Many existing formats for spatial data, however, are complex to split and parse. RDBMS with spatial extensions usually handle *well-known text* (WKT) and *well-known binary* (WKB) [42] geometries contained inside comma or tab separated files. This makes splitting the data a case of searching for newlines in the dataset. Public spatial datasets, however, tend to favour more structured data formats, such as XML [43] and JSON [8], in order to simplify interoperability. These semi-structured formats do not have the same ease of splitting as database bulk formats.

As a result, we focus on *GeoJSON* [19] because it encompasses many features that make parallel processing challenging, such as a recursive definition and support for arbitrary metadata. An example fragment is given in Listing 1. Allowing geometries to contain other geometries prevents splitting based on hierarchy; supporting free-form user metadata makes splitting using known strings unsound—without full parsing, it is impossible to decide if the string indicates a hierarchy boundary or is part of the metadata. We also consider WKT- and XML-formatted data to show the flexibility of our approach in handling different input formats.

2.3 Existing solutions

Spatial DBMS. Both relational and NoSQL-style database engines have added spatial query support: *Oracle* [45], *Microsoft SQL-Server* [15] and *IBM DB2* [9] all offer spatial extensions, as well as several open-source engines, including *PostGIS* [25] and *MySQL* [39]. RDBMS support spatial data through the use of spatial indexes, such as *R-trees* [40] (used by PostGIS) or *Quadtrees* [32] (available in Oracle). These index structures operate on the bounding boxes of geometries, providing an efficient mechanism to select possible matches. Each possible match still needs to be refined by comparing the geometries, a process often taking longer than the index search [54]. There is also the upfront cost of creating the index, which may dominate for regularly updated datasets.

In contrast, the *MonetDB* column store [59] does not have a spatial index but instead stores bounding boxes as a separate column [38]. The rationale is that the sequential access pattern of scanning a column offsets the extra computation due to the lack of an index. MonetDB can parallelise some operations, but spatial joins are sequential and require constructing the entire candidate set in memory. For containment queries, sequentially laid-out bounding boxes can achieve performance comparable to indexes for pre-filtering. This approach fails to scale to large joins because it requires sufficient memory to hold the product of the joined columns.

GeoCouch [18] supports simple filtering primitives for the CouchDB NoSQL datastore [3]. There is no join support, and the performance has so far been shown to be up to $3\times$ worse than PostGIS on a single node [37]. By sharding documents across nodes, it may be possible for GeoCouch to scale, but this has yet to be demonstrated for geospatial data. GeoCouch also has the fewest supported spatial query operators of any of the discussed systems.

Distributed frameworks. The two main implementations for spatial query processing on clusters are *Hadoop-GIS* [1] and *SpatialHadoop* [13], which are both based on the Hadoop map/reduce framework [10]. While both systems perform data indexing, Hadoop-GIS assumes that index creation is inexpensive and thus can be done mostly on demand, with only the largest regions indexed statically. while SpatialHadoop is more concerned with up-front indexing. Despite the indexing support of these systems, we show that AT-GIS achieves substantially better performance without prior indexing.

Any system built on top of Hadoop requires that the data is first loaded into the HDFS distributed file system with suitable partitioning. Both systems use spatial partitioning to distribute objects between nodes. Given that an object can be part of multiple spatial partitions, each system must have a way to either eliminate duplicate objects or transfer them between nodes: Hadoop-GIS spends substantial time on boundary handling—objects are duplicated prior to parallel processing and then duplicate results are pruned; SpatialHadoop uses more sophisticated indexing structures to avoid this in most cases. While AT-GIS supports partitions similar to Hadoop-GIS, following a *partition-based spatial merge join* strategy [48], its single-node design eliminates expensive network I/O.

Discussion. All of the above approaches for spatial query processing require that the input data is loaded first so that indexing or partitioning can be performed. Once loaded, the data is processed in parallel using the internal data structures to create independent work units. An important requirement for a system with a low data-to-query time, however, is that it operates in parallel from the start, without assuming the existence of any ancillary data structures.

A related requirement is for the data to be left in its original form. A conversion of data into an internal representation requires at least two data passes: one pass to do the conversion, and a second pass to perform the query. For loaded data, a more compact representation may be used, which reduces I/O bandwidth for queries such as joins that require multiple passes of the data on disk; for single-pass queries, however, this may increase I/O bandwidth usage.

Finally, the system should operate on a single node in parallel. For current map/reduce-based cluster systems, significant inter-node communication is necessary during the reduce phase to handle geometries that straddle partition boundaries. By confining computation to a single multi-core node, this deduplication can be handled internally rather than being limited by the network bandwidth.

3. ASSOCIATIVE TRANSDUCERS

To execute spatial queries with a single data pass, we need a computational model that is expressive enough to represent the whole processing pipeline for spatial queries, from the parsing of the raw spatial data to the execution of spatial operators. The model must also be parallelisable and should have bounded internal state.

While *transducers* [36] have primarily been used for lexing and parsing, we introduce a new transducer class, called *associative transducers*, that can express a wide range of spatial query operations. Transducers are an inherently sequential model, but we show that, through a combination of *speculation* [41] and the properties of our new transducer class, it becomes possible to construct pipelines of transducers that can execute spatial queries with data parallelism.

First we provide a formal description of associative transducers and show how they support data-parallel operations (§3.1) while maintaining the property of compositionality required to construct complex spatial query processing pipelines (§3.2). After that, we discuss the specific types of transducers needed to support spatial querying (§3.3) and how they map to spatial query operators (§3.4). Finally, we introduce *partially-associative transducers*, an optimisation that reduces the overhead of speculation (§3.5).

3.1 Formal description

We assume a transducer T can be represented as a five-tuple $T = (Q, q_0, \Sigma, \Gamma, \delta)$ where Q is the set of states, q_0 is the starting

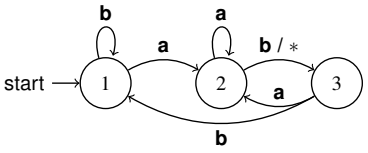

Figure 1: Transducer for matching the string ab

state, Σ is the input alphabet, Γ is the output alphabet, and δ is the transition function. We only consider deterministic transducers, making δ a function of the current state and input symbol. We do not require that Q is finite to ensure that the model can express both aggregations across infinite sets and pushdown transducers.

If we combine the state Q and output tape Γ^* of a regular transducer into a pair $p \in P = (Q \times \Gamma^*)$, we can think of execution as an operator $p \odot s \to p'$ where s is an input symbol. $\odot$ is defined as performing the state transition of T and updating the output tape. The result of processing T on a string of symbols $s_1, s_2, \cdots, s_i$ is the same as $p_0 \odot s_1 \odot s_2 \cdots \odot s_i$ where $p_0 = (q_0, \varepsilon)$. $\odot$ is clearly non-associative because it cannot operate on two symbols, relying on a left-reduction to be well-formed.

An *associative transducer* (AT), denoted as T', is a generic construction over T to support associative operations. We wish to be able to define a function $\otimes$ that has the same semantics as $\odot$ but supports associative reduction. We define ATs as having *fragments*, rather than states. A fragment f' contains a *state mapping relation* $q' \in Q' : [Q \to Q]$ that maps potential starting states to corresponding finishing states, where Q' is the set of all such relations. A fragment also contains a set of predicated output tapes $o' \in [Q \to \Gamma^*]$ to store the symbols emitted by the transducer. The predicates are needed because some output symbols may only be emitted for a subset of possible starting states.

The state mapping relation begins as the identity relation. As symbols are processed, each entry in the fragment has its finishing state updated. Merging two fragments results in the composition of the two relations. As the composition of relations is associative, the action of the AT is also associative.

Using these definitions, we can now define an operator $\bigcirc$:

$$(q', o') \bigcirc s_i \to \left(\begin{array}{ll} \{(q_i, q^*) & \mid (q_i, q_f) \in q' \text{ and } q^* = \delta_Q(q_f, s_i)\}, \\ \{(q_i, o : o^*) & \mid (q_i, o) \in o' \text{ and } (q_i, q_f) \in q' \text{ and} \\ & \quad o = \delta_\Gamma(q_f, s_i)\} \end{array} \right)$$

where : is string concatenation, and δ_Q and δ_Γ are defined such that $\delta(q, s_i) = (\delta_Q(q, s_i), \delta_\Gamma(q, s_i))$.

We now transform each symbol in the input into a fragment independently. We also define a function $\otimes$ to merge fragments:

$$(q'_1, o'_1) \otimes (q'_2, o'_2) \to \left(\begin{array}{ll} q'_1 \circ q'_2, & \\ \{(q_s, o_1 : o_2) & \mid (q_s, o_1) \in o'_1 \text{and} \\ & \quad (q_s, o_2) \in q \circ o'_2\} \end{array} \right)$$

where $\circ$ is relation composition. As this function depends only on relation composition and string concatenation, which are both associative operations, the resulting merge function is also associative.

Rather than two relations, the fragment can be considered equivalently as a *fragment function*, which takes a starting state and returns the corresponding finishing state and output tape. Using this model, we can find efficient ways to represent the fragment function other than storing the relations directly (see §3.3).

Example (Matching transducer): Consider the simple string transducer in Fig. 1 that outputs $*$ each time the string ab is seen. To operate on the string abab, we split the string into individual symbols and construct execution pairs for each one:

Input	a	b	a	b
Fragment	$\{1,2,3\} \to 2$	$\{1,3\} \to 1$ $\{2\} \to 3$	$\{1,2,3\} \to 2$	$\{1,3\} \to 1$ $\{2\} \to 3$
Output		$\{2\} \to *$		$\{2\} \to *$

The symbol b results in an execution pair that outputs a single $*$ if the actual starting state turns out to be 2, but not if the starting state was 1 or 3. The next step is to combine the pairs associatively:

Input	ab	ab
Fragment	$\{1,2,3\} \to 3$	$\{1,2,3\} \to 3$
Output	$\{1,2,3\} \to *$	$\{1,2,3\} \to *$

These intermediate results show the property of *convergence*: the number of distinct finishing states in the relation decreases as data is processed. Since the transducer is deterministic, the number of distinct finishing states in a fragment cannot increase.

The final step is to merge the remaining two execution pairs to compute that, regardless of the starting state, the finishing state is 3, with $**$ on the output tape.

3.2 Composition and parallel execution

By storing fragments for the next transducer in a pipeline, rather than the output tape, we can compose multiple ATs. We observe that the string concatenation operator : can be replaced by any associative operator $\otimes$ without invalidating the transformation. When two ATs are combined, the first transducer now stores a predicated set of fragments from the second transducer, rather than the output tapes. This model can be extended to a pipeline of arbitrary length.

One possible way of parallelising a pipeline would be to execute each stage concurrently, but this would limit the degree of parallelism to the number of transducers in the pipeline and require synchronisation to pass data between them. Instead, the pipeline can be executed in a *data-parallel* fashion, constructing fragments independently for blocks of data that can then be merged together. This provides greater parallelism, which is better suited to achieve scalable query processing with many CPU cores.

Example (Counting transducer): Building on the previous example, to count the number of $*$ symbols on the tape, we can construct a simple counting transducer with $Q = \mathbb{N}$, which increments when a $*$ is seen as input. We then compose the two transducers to count the occurrences of ab. Using the same string and the matching transducer as before, we can see below that, under b, a 1 is contained in the predicated list and a 0, otherwise.

Input	a	b	a	b
Fragment	$\{1,2,3\} \to 2$	$\{1,3\} \to 1$ $\{2\} \to 3$	$\{1,2,3\} \to 2$	$\{1,3\} \to 1$ $\{2\} \to 3$
Output	$\{1,2,3\} \to 0$	$\{1,3\} \to 0$ $\{2\} \to 1$	$\{1,2,3\} \to 0$	$\{1,3\} \to 0$ $\{2\} \to 1$

The execution proceeds analogously to the previous example except that, instead of concatenation, we add the fragments of the counting transducer. The result is that, regardless of the starting state, the finishing state of the matching transducer is 3, with 2 as the fragment of the counting transducer.

3.3 Spatial query processing

Next we explore efficient implementations of the fragment function for different types of transducers needed for spatial query processing. We identify five types of ATs that can be mapped to operations when processing spatial data:

1. *finite state transducers* for lexing the input data;
2. *deterministic pushdown transducers* for extracting the data and metadata from lexed symbols;
3. *stateless transducers* for conversions on points or aggregates;
4. *aggregation transducers* for summarising data; and
5. *periodically flushing transducers* for aggregating geometries.

We look at each in turn, grouping the conceptually similar finite and pushdown transducers together along with the stateless and aggregation transducers. To illustrate the use for each type of trans-

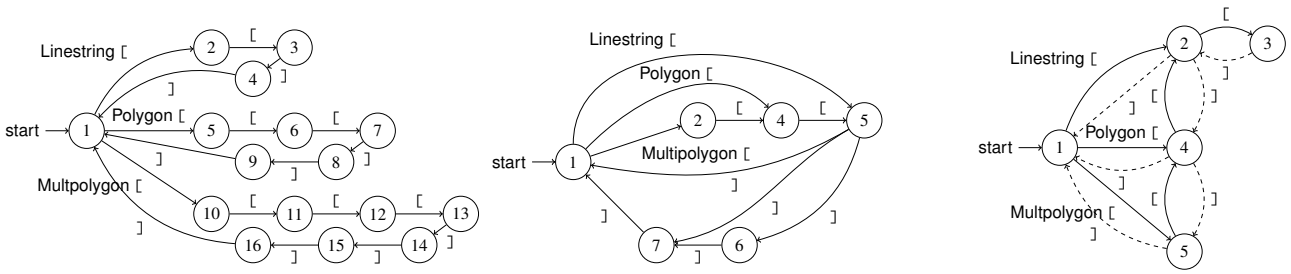

(a) Deterministic transducer (b) Non-deterministic transducer (c) Pushdown transducer

Figure 2: Three potential automata for parsing geometries

ducer, as a running example, we consider all of the stages required to divide the shapes from GeoJSON data into spatial partitions.

Finite and pushdown transducers can extract spatial data from a raw format. Finite transducers have an explicit associative form: each fragment contains the state mapping relation from all possible starting states to the corresponding finishing states and a set of output tapes predicated by the starting states. When an input symbol is processed, each entry in the relation is updated, and output symbols are appended to the output tapes.

A natural way to express these relations are as $N \times N$ binary matrices, where N is the number of states in the transducer. For a small number of states, the transitive closure under multiplication can be precomputed as a set of lookup tables. This is similar to the approach used by *simultaneous finite automata* [56] but with the addition of an output tape.

Each output tape in the fragment has a predicated set of starting states represented by a vector. By considering all output tapes formed as a vector, a matrix can be used to associate starting states with corresponding output states. The complete fragment thus holds a state relation mapping matrix, an output matrix and a vector of output tapes. This representation allows for tapes to be shared among multiple starting states after convergence was achieved.

All of the relation composition operations needed to merge execution pairs thus become precomputed matrix multiplications. Merging the output tapes from each pair thus becomes the dominant factor in performing merges. This is mitigated by limiting the number of possible starting states based on the structure of the lexer. For example, in XML, it can be guaranteed that if a block starts with a `<` character, there are only three possible starting states (comment, `CDATA` or neither); the **,** character in JSON can fulfil a similar purpose. This can only be done without impacting performance if the searched character is common in the input stream [41].

It is possible for the same parsing task to be implemented using different automata models. Fig. 2 shows the transition diagrams of parsers for a simplified geometry format based on GeoJSON. A deterministic finite transducer requires fewer states than either a non-deterministic or a pushdown transducer (Fig. 2a). As the cost of speculation depends on the number of states, and we do not have a formal model for a non-deterministic transducer (Fig. 2b), we choose to implement the parsing of spatial data formats using pushdown transducers (Fig. 2c).

Stateless and aggregation transducers. The stateless (SLT) and aggregation (AGT) families of transducers correspond to the functional *map/filter* and *reduce* primitives found in parallel processing [10, 26]. They are used to support mathematical and spatial transformations and aggregations in spatial queries. We exploit their associativity to provide efficient AT implementations.

A stateless transducer is one for which the set of states Q is a singleton $\perp$, i.e. there is no shared state carried over between input symbols, and each can be processed independently. The transition

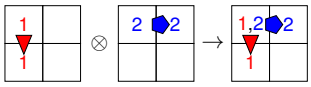

Figure 3: Partitioning expressed as an associative operation

function δ thus takes the form $\delta(\perp, s) \to (\perp, p(s))$ where $p : \Sigma \to \Gamma^*$ is the mapping function. Each input can result in zero or more outputs, giving it the expressive power of both *map* and *filter*. A stateless transducer has a trivial associative form without any state to manage. For example, coordinate space conversion—a common operation in spatial querying—can be done by stateless transducers.

Example (Point parser): A point parser is a transducer that takes streams of point offsets and produces a stream of point values. It is used to isolate the structural parsing, performed by finite and pushdown transducers, from handling floating point values. It is stateless as each offset can be parsed into a point value independently, with no dependencies between adjacent symbols in the input data.

Aggregation transducers perform some reduction over the input data without producing output. The reduction function combines the internal state of the transducer with the input value to produce the new internal state. More formally, an aggregation transducer has a transition function $\delta(q, s) \to (a(q, t(s)), \varepsilon)$ where the *transformation function* $t : \Sigma \to Q$ converts each input symbol into a state, and an *aggregation function* $a : Q \times Q \to Q$ combines states.

An efficient AT relies on the properties of the aggregation function: if the function is associative, the transformation only needs to store one copy of the in-order state to reconstruct the whole state relation. If the aggregation function is not associative, another approach is needed, typically buffering until the aggregation can be run in-order. Aggregations can be numeric, e.g. when computing the sum of values, or spatial, e.g. when computing the set-theoretic union of a list of shapes.

Example (Partition): Spatial partitioning is an example of an operation that can be performed by an aggregation transducer. The state of the transducer contains a set of spatial partitions and the identifiers of the contained objects. Fig. 3 shows two partitions, each containing a single object numbered 1 and 2. The associative merge operation ($\otimes$) concatenates the list of objects in each partition.

Periodically flushing transducers are a hybrid of stateless and aggregation transducers and can perform aggregations over subsets of the input stream, e.g. computing a bounding box for each geometry.

The set of input symbols can be divided into two disjoint sets: P for processing symbols and F for flushing symbols. When a flushing symbol is received, zero or more output symbols are emitted, and the internal state resets to the starting state q_0; when a processing symbol is received, the internal state is updated but no symbols are output. Thus periodically flushing transducers perform aggregations on strings of processing symbols demarcated by flushing symbols. The processing symbols are typically points or edges, and the flushing symbols are markers for geometry boundaries.

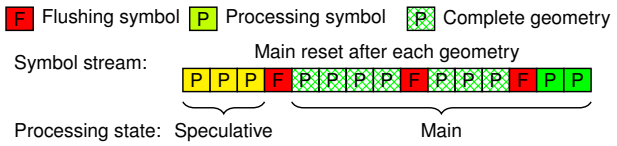

Figure 4: Data processing with a periodically flushing transducer

As with aggregation transducers, the most efficient transformations into an associative form arise when the aggregation function is itself associative. In this case, the fragment of an AT can be represented using two copies of the in-order state: the *speculative* and *main* states. Fig. 4 shows the speculative state that is used to aggregate the processing symbols before the first flushing symbol, while the main state is used for all input symbols from that point on. An additional bit is needed to record if at least one flushing symbol was seen and hence which copy of the state should be used for processing the next input symbol. Only one output tape is needed to store the results of the main state. The output from the speculative state is not determined until merging.

To merge two associative fragments, the main state at the end of the first must be merged with the speculative state at the beginning of the second. The result is a new aggregation that must be inserted into the output tape between the tapes of the two merged fragments.

Example (Polygon bounding): A periodically flushing transducer can compute the master bounding rectangles (MBRs) of geometries. The processing symbols are the point values, and the flushing symbols are the special values marking the boundaries of geometries. MBR computation from a list of points is an associative operation as each point can be considered as its own bounding box, and an associative operation computes the union of the boxes. Merging can similarly be performed by computing the spatial union of the two partial states being merged.

3.4 Support for spatial operators

Next we consider a set of spatial operators and describe how each can be expressed as an AT. We first explain the case in which operators are used as a predicate with a single or small set of objects provided as a query parameter, and then describe how the operators can be used for joins. Finally, we address extensions, as used by PostGIS and other spatial DBMS, to provide geometry aggregation.

We focus on the spatial operators provided by the SQL option of the *Open Geospatial Consortium Simple Feature Access Specification* [42] when comparing polygons to polygons, as listed in Table 1. We split the operators into three categories: operators that (i) calculate some property on a single geometry; (ii) spatially relate two geometries; and (iii) represent set-theoretic operations on one or more geometries. Table 1 shows the mapping into transducers when one of the operands is a query parameter. We consider the case in which operators are used in a join query separately.

For each operator, we state the input and output types of the corresponding transducer as well as the type of any internal state. The class of each generated transducer (from §3.3) is also listed along with the corresponding associativity available. The most flexible form of associativity is "in shape", which allows a single shape to be distributed; "between shapes" requires that each shape is allocated to a single thread, potentially reducing parallelism.

The first category of operators contains those that operate on a single geometry to perform some form of aggregation. With the exception of `ST_IsSimple` and `ST_Boundary`, both of which must consider the geometry in its entirety, the others can be implemented as PFTs, constructing a partial aggregation and merging the two. We have already explored the case of bounding box calculation as part of the running example in the previous section.

Spatial operator	*Input*	*Output*	*Processing state*	*Transducer class*	*Associativity*
		(i) Single geometry properties			
`ST_IsEmpty`	Points	Bool	Bool	PFT	In shape
`ST_IsSimple`	Shapes	Bool	None	SLT	Between shapes
`ST_Envelope`	Edges	Boxes	Box	PFT	In shape
`ST_ConvexHull`	Points	Shapes	Shape	PFT	In shape
`ST_Boundary`	Shapes	Shapes	None	SLT	Between shapes
		(ii) Geometry relations			
`ST_Disjoint`	Edges	Bools	Bool×Bool	PFT	In shape
`ST_Intersects`	Edges	Bools	Bool×Bool	PFT	In shape
`ST_Touches`	Edges	Bools	Bool	PFT	In shape
`ST_Crosses`	Edges	Bools	Bool	PFT	In shape
`ST_Within`	Edges	Bools	Bool×Bool	PFT	In shape
`ST_Contains`	Edges	Bools	Bool×Bool	PFT	In shape
`ST_Overlaps`	Edges	Bools	Bool×Bool	PFT	In shape
`ST_Relate`	Edges	Relations	Relation	PFT	In shape
`ST_Distance`	Edges	Floats	Float	PFT	In shape
		(iii) Set-theoretic operations			
`ST_Intersection`	Shapes	Shapes	None	SLT	Between shapes
`ST_Difference`	Shapes	Shapes	None	SLT	Between shapes
`ST_Union`	Shapes	Shapes	None	SLT	Between shapes
`ST_SymDifference`	Shapes	Shapes	None	SLT	Between shapes
`ST_Buffer`	Shapes	Shapes	None	SLT	Between shapes

Table 1: Representation of spatial operators as ATs

The second category includes all those operations that perform some spatial relation. When comparing against a known reference set, these operators can be executed using an algorithm that compares each edge in turn. Using `ST_Intersects` as an example, we use an edge testing algorithm that compares each incoming edge with the edges in the reference set. Any crossing means that the geometry intersects with the reference. To handle the case in which one polygon is entirely inside another, we perform two point-in-polygon tests, one comparing the first point in the geometry against the reference set and the second comparing an arbitrary point in the reference set against the geometry. If either of these two tests matches, the geometries are intersecting.

The final category includes set-theoretic operations on shapes. As such operations require processing the entire polygon as a single entity rather than each point or edge individually, we cannot use a PFT. Instead we use transducers that operate on a stream of polygons as stateless transducers when each operation is independent, e.g. using `ST_Buffer` on a stream or `ST_Difference` on a stream of joined pairs or with a reference object. Alternatively, when the operator is used as an aggregation across a column, e.g. using `ST_Union` on a large set of geometries, we can take advantage of the associativity of set operations to use an aggregation transducer.

When a spatial predicate is used for a join between two large sets of geometries, the model used for a small reference set ceases to be effective, requiring an alternative approach. Typically some version of a plane or line-sweep algorithm can be used. Our transducer model is not a good fit for a join between two data streams, so we wrap the join into a transducer that takes sets of shapes as input and emits joined pairs as the output stream. This permits the use of transducer operations before and after the join, while having the performance of existing parallel joins. We use a *partition-based spatial merge join* [48] to perform all spatial joins between two datasets, using transducers for the initial partitioning.

3.5 Partially associative transducers

Depending on the input data, it may be possible to relax the requirement for full associativity to reduce speculation. *Partially-associative transducers* are an optimisation when the data can be split in such a way that the state at the start of a block is known. This is common in many spatial data formats, even recursive ones such as GeoJSON, if the complete schema is known in advance.

The idea for this optimisation is to introduce some logic into the splitting of the data into blocks such that block boundaries occur only at locations that result in known states: in comma- or tab-separated text files with no escaping, this is typically the end of

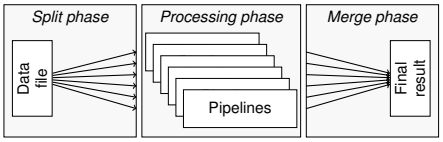

Figure 5: Phases of pipeline execution in AT-GIS

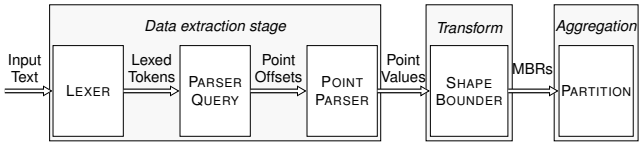

Figure 6: Pipeline for shape partitioning in a textual data format

lines; in XML or JSON, it is commonly some tag that only appears at a given point in the hierarchy and that can be used to establish the state of the parser for the block.

In some cases, it may be possible for the tag to appear at an unexpected location due to a free-form field in the input. A partially-associative transducer may then temporarily process the data incorrectly, but the inconsistency will be caught during a subsequent merge. The data would then have to be reprocessed, but it would not affect the correctness of the final result.

Example (GeoJSON parsing): For GeoJSON, the parse and querying stages can be converted into a partially-associative form by exploiting the object type field that appears within each object. If object boundaries can be found, the lexer and parser can be started in a known state, permitting the use of an optimised, off-the-shelf library without speculation. For example, it is possible to use a regular expression to search for the string `"type":"Feature"`, as seen on line 3 in Listing 1. Since the tag is not necessarily the start of an object, a parser can find the boundaries of the object.

4. AT-GIS DESIGN

In this section, we describe how AT-GIS uses associative transducers (ATs) to create parallel processing pipelines for the execution of spatial queries. First we introduce its processing model (§4.1) and present the pipelines for different query types (§4.2), explaining their physical query plans, how stages are decomposed into ATs and how the system is implemented (§4.3). After that, we focus on each pipeline stage in turn, exploring the trade-offs for performance optimisation (§4.4). We finish with a discussion of spatial joins and how they use multiple pipelines (§4.5).

4.1 Overview

AT-GIS executes spatial queries by translating a *physical query plan* into *pipelines* of transducers. The physical plan takes the form of a dataflow representation of the query [53] in which the majority of spatial operators are compiled into a single pipeline. Joins require multiple pipelines because they rely on barriers.

The construction of the physical query plan follows past work on optimising pipelined parallel query execution [6]. AT-GIS assumes a tree-shaped dataflow graph in which each spatial operator is represented by a node; edges denote the objects transfered between operators. AT-GIS supports a hierarchy of four object types, with *points* being the lowest level, followed by *edges*, *rings* and *polygons*. In general, edges should be typed with the lowest-level object supported by both sides—the lower the level, the greater the opportunity for parallelism. All but conditional and join operators have a single input and output edge.

AT-GIS then constructs a pipeline from each linear section of the dataflow graph. It makes special consideration for conditional operators (§4.4.2) to allow them to form part of a linear pipeline in spite of them not being linear. Once the pipelines have been defined, AT-GIS compiles them using an optimising compiler to reduce the overhead of the abstraction between stages.

As shown in Fig. 5, the execution of pipelines involves three *phases*: *split*, *processing* and *merge*. The split phase divides the input data into blocks. Data splitting may require incrementing a pointer (for fully-associative transducers) or executing a regular expression and lightweight parsing (for partially-associative transducers). After a data block is formed, it is placed in a work queue for the processing phase. The processing phase performs the majority of the computation by passing blocks from the work queue through the pipeline. As ATs make the tasks independent, it can be scaled to many parallel threads. The merge phase combines all of the partial results from the processing phase to compute the final query result. While the first two phases can run concurrently to reduce latency, the third phase executes only after all blocks are available.

4.2 Spatial query processing pipelines

Fig. 6 shows how a single-pass pipeline can be split into three logical *stages*: (i) parsing of the dataset and extracting the data of interest; (ii) transforming and filtering the data to answer the query; and (iii) aggregating the result. The *parsing/data extraction* stage is responsible for consuming bytes from the input file and outputting a stream of point values. If required by the query, any filtering on the metadata is also handled by this stage. Restricting metadata queries to the first stage ensures that format-specific knowledge is not needed in the rest of the pipeline. The *transformation/filtering* stage encompasses any operations that process individual geometries or points and consists primarily of periodically flushing transducers. Finally, the *aggregation* stage performs any aggregation across all the geometries. In the case of a containment query, the final stage buffers the result for output.

Each object between pipeline stages is tagged with the data offset from which it was created. Offsets are used in two ways: to enable unique identification of points and geometries; and to allow reparsing of objects in the join pipeline. The type of the objects transfered between the transformation and aggregation stage depends on the nature of the aggregation: spatial aggregations require that the aggregation stage receives all point data, whereas numeric aggregations require only the computed result.

4.3 Pipeline implementation

Each pipeline stage is written as a C++ class template with the template parameter describing the destination for output symbols. Pipelines are thus constructed back to front, starting with the final aggregation transducer before wrapping it with the previous stages.

Using templates to perform composition rather than more commonly seen indirect function calls has two advantages: (i) there are no restrictions on the types of symbols that are passed between stages; and (ii) an optimising compiler can combine stages, using inlining to remove most of the overhead of passing symbols along the pipeline. Inlining also allows for general-purpose optimisations, such as loop unrolling, to be performed across multiple stages.

The disadvantage of a template-based approach is that the pipelines have to be known at compile time. For this reason, AT-GIS generates and compiles a pipeline prior to executing the query, creating an executable that can then be run on the raw data. While compiling templated C++ code adds some overhead compared to a traditional database engine, we show in §5.1 that the total query execution time is still much reduced compared to existing systems.

4.4 Pipeline stages

Next we describe the details of each stage. Although the structure of the pipeline is fixed for a given query, there are possible data- and query-dependent optimisations within each stage.

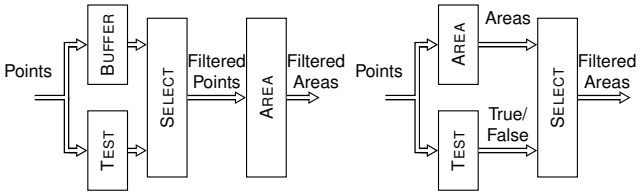

(a) Buffered (b) Streaming

Figure 7: Pipelines for selecting geometries

(1) Parsing/data extraction stage. This stage converts the input format into a list of spatial primitives suitable for the rest of the pipeline. AT-GIS supports spatial queries over GeoJSON, WKT and OpenStreetMap XML data. WKT is the most straightforward to support because it is mostly a non-nested (except for `GeometryCollections`) text-based format with all of the point data available inside the shape objects. GeoJSON adds an extra layer of complexity by allowing arbitrarily formatted metadata within the object. It thus needs a push-down parser to understand the format correctly.

OpenStreetMap XML is the most complex format to support because it separates the data into multiple sections: first it lists all the *nodes* that link a numeric identifier to a point in space; followed by the *ways* that relate multiple nodes; and finally *relations* that link nodes and ways to describe complex polygons. AT-GIS handles the separation of point and polygon data by keeping a temporary table of all points and ways on disk, which is constructed during the first data pass. When ways and relations are processed in subsequent passes, the need to re-parse the data from source is reduced.

In general, the parsing stage may use fully- or partially-associative transducers. As we show in §5.5, the type of transducer that achieves the highest throughput depends on properties of the data. Since this is not known in advance, AT-GIS leaves the selection to the user.

With partially-associative transducers, the parsing stage consists of a wrapper around an off-the-shelf parser, which inputs well-formed data blocks and outputs the stream of points, potentially filtered by some metadata. Where possible, AT-GIS uses streaming parsers, e.g. using the SAX API [55], to limit memory usage.

Fully-associative parsers are constructed from the finite and push-down transducers. For all of the supported input formats, i.e. GeoJSON, WKT and XML, AT-GIS separates the lexing and parsing and employs transducers suited for each task.

Lexing is handled by finite transducers optimised for small transition tables. As a transition must be performed after each byte, precomputation is used for all the transition tables, which reduces the overhead of the associative construction. As explained in §3.3, we use pushdown transducers to perform parsing and data extraction to reduce the required speculation.

In addition to extracting geometry and point offsets, any filtering on the accompanying metadata is also compiled into the parsing automaton. As pushdown transducers can handle XPath-style queries [49], AT-GIS supports a similar query language for JSON that filters on the structure or value of fields in the metadata.

In typical scenarios, such as our running partitioning example, the execution time of the pipeline is dominated by the parsing/data extraction stage. While exact numbers are difficult to obtain because the optimising compiler merges stages together, at least 90% of the CPU time is spent in this stage.

(2) Transformation/filtering stage. The second pipeline stage consists of periodically-flushing transducers that wrap standard geometric algorithms. AT-GIS converts between streams of edges and points to match the requirements of the algorithms. Most supported algorithms are edge-centric, such as perimeter and area calculations, and only a small number, e.g. MBR calculations, are point-centric.

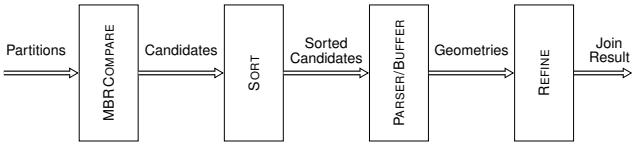

Figure 8: Join pipeline

An operation that conflicts with the requirement to perform the least amount of buffering is selecting geometries for which the point data is required later in the pipeline. An example is finding the areas of all geometries within a defined region. AT-GIS has two ways to construct a pipeline for such queries, trading off buffering against redundant computation: (i) in a buffered approach (see Fig. 7a), the geometry is stored until the result of the inclusion test is known; and (ii) in a streaming approach (see Fig. 7b), the area is computed at the same time as when the test is performed.

The most effective approach depends on the query selectivity, the expected size of the largest geometries, and the cost of the aggregation. For non-selective queries, all of the computation is necessary, so the additional buffering only adds memory overhead. For highly-selective queries, the cost of unnecessary computation outweighs the buffering overhead. We explore these trade-offs in §5.4.

(3) Aggregation and partitioning stage. The final stage in the single-pass pipeline performs aggregation. While required for aggregation queries, it is also used for containment queries to store the output of the transformation stage before returning the result.

While AT-GIS supports both spatial and numerical aggregation, it only maps numerical aggregation directly into the pipeline. Numerical aggregation consists of operations such as `sum` and `avg`, which can be mapped easily to an associative form. Spatial aggregations are operations such as spatial unions for which we have not developed a suitable associative form—AT-GIS executes them as a separate sequential phase after the executation of the pipeline.

A special form of aggregation is *partitioning*, which terminates the first pipeline when performing a spatial join. By having to concatenate multiple lists during a merge, partitioning does not have the constant-time merge property of numerical aggregations.

AT-GIS supports two data structures for partitions: arrays and linked lists. Arrays have better memory locality and a lower memory footprint at the expense of linear-time merging; linked lists achieve constant-time merging but with slower access due to cache-unfriendly patterns. To reduce the cost of merging many partitions, it is possible to perform the partitioning as a sequential step after the processing pipeline. This requires that only one list or array is merged for each block, rather than one per partition and block.

An important parameter to choose is the number of partitions. It determines the available parallelism in later processing, so a large number is desirable to improve e.g. join performance. Many partitions, however, increase the merging cost of the results of the first stage and lead to unnecessary computation when more geometries straddle partition boundaries. In §5.6, we explore this parameter choice with a large, real-world dataset.

4.5 Spatial joins

When a spatial join is part of a query, AT-GIS constructs a second pipeline that consumes partitions and emits the joined geometries. This pipeline uses a set of specialised transducers to implemented a PBSM join algorithm [48]. This permits the join to execute alongside other transducers if further selection or aggregation is needed. Since the partitions are non-disjoint, there is a possibility of duplicate results in the output, which are removed by a sequential step prior to returning the query result.

The PBSM join is realised as a *join pipeline* of ATs, operating on the spatial partitions (see Fig. 8). The partition has two lists of

Name	*Description*	*Size (GB)*	*Shapes (1000s)*
OSM-X	OpenStreetMap XML	592	187,560
OSM-G	OpenStreetMap GeoJSON	63.3	187,560
OSM-W	OpenStreetMap WKT	41.0	187,560
OSM-10G	OpenStreetMap replicated	633	1,875,600
Synth$_{n,\sigma}$	Synthetic dataset	10.0	n/1000

Table 2: Spatial datasets used for evaluation

MBRs and the offset in the original data of the corresponding object. Storing the offsets means that objects can be re-parsed on demand, avoiding the need to keep the entire dataset in memory.

The join pipeline first finds all MBR intersections in a partition (MBR COMPARE transducer) and passes a stream of potentially matching candidates to the SORT transducer. SORT buffers the stream until a threshold is reached, and then sorts the objects by location in the input data. The aim is to position candidates involving the same objects adjacently so that the time that objects remain in memory is bounded. As adjacency can only be achieved for one of the two sets of objects being joined, AT-GIS makes the largest set adjacent. The PARSER/BUFFER transducer re-parses objects to construct the full geometry for refinement. A hash map stores objects in the non-adjacent stream to limit repeated parsing. Once a block is processed, the hash map is cleared. Finally, the REFINE transducer performs the join test, such as geometry intersection.

Storing entire objects in memory can potentially exhaust available resources. By adjusting the threshold in SORT, the number of stored objects can be reduced. While reducing memory usage, some objects may have to be read several times when the entire partition cannot be processed as a single sorted block.

As objects can appear in multiple spatial partitions, duplicate matches may be part of the final result. To mitigate this, after the join pipeline has finished, AT-GIS sorts the result by the offsets of both objects joined and eliminates duplicates.

If additional processing is required on the joined objects, this can either be added to the end of the join pipeline or as a separate phase after duplicate elimination. As objects are only retained in memory while needed by the pipeline, running algorithms as a separate stage may require objects to be re-parsed. Executing computation inside the pipeline provides immediate access to the joined objects at the expense of potentially encountering duplicate results, which need to be removed.

5. EVALUATION

We evaluate AT-GIS experimentally: we compare its performance against other approaches (§5.1) and use synthetic and real-world datasets to explore scalability (§5.2), different data formats (§5.3), different filtering pipelines (§5.4), dataset skew (§5.5) and partitioning options (§5.6).

Datasets. Table 2 summarises our datasets. We use the OpenStreetMap dataset [44], retrieved on May 18, 2015. This is a large real-world dataset that is widely used to benchmark spatial query processing. In addition to the orignal XML file (OSM-X), we prepare two additional versions: a GeoJSON-formatted one (OSM-G) and a WKT-formatted one (OSM-W), which is used for loading into PostGIS, MonetDB and SpatialHadoop. We also create a version in a proprietary format of a commercial DBMS. In addition to the geometry, we add an object `id` into each object as metadata.

To evaluate scalability as the data sizes grow beyond the available memory, we create a larger dataset (OSM-10G) by replicating the OpenStreetMap dataset 10 times. For each replication, the geometries are kept the same but the `id` is changed to ensure uniqueness.

We also generate a synthetic dataset (Synth) that includes polygons and multi-polygons with the number of edges distributed according to a log-normal distribution. Two parameters control the number of geometries and the σ value of the distribution. The size of the geometries is scaled so that the dataset is 10 GB.

Query	*SQL*
Containment	`SELECT * FROM data WHERE ST_Intersects(geom, ref)`
Aggregation	`SELECT ST_Area(geom), ST_Perimeter(geom) WHERE ST_Intersects(geom, ref)`
Join	`SELECT * FROM data d1, data d2 WHERE d1.id < threshold AND d1.2 > threshold AND ST_Intersects(d1.geom, d2.geom)`
Combined	`SELECT ST_Area(ST_Union(d1.geom, d2.geom)) FROM data d1, data d2 WHERE ST_Perimeter(d1.geom) > t1 AND ST_Perimeter(d2.geom) < t2 AND ST_Intersects(d1.geom, d2.geom)`

Table 3: Spatial SQL queries used for evaluation

Queries. We use four types of spatial SQL queries, as shown in Table 3: a *containment* query that selects all polygons contained within some bounding box; an *aggregation* query that combines containment with a summary function over all of the matching polygons—in our case, we use the total perimeter and total area; a *join* query for which we split the input data into two disjoint subsets and which finds all intersecting pairs; and, finally, we use a *combined* query to show how AT-GIS handles more complex pipelines consisting of two containment queries to determine the input to a join, followed by an aggregation on the resulting pairs. Experiments with queries that use other geometries and predicates give similar results.

As our input data is geographic, we perform all of our computation using a spherical coordinate system. We use two methods to calculate the linear distance between points when performing perimeter calculations: by default, we use spherical projection, but, in §5.4, we also employ the more accurate but more expensive computation using Andoyer's algorithm [4].

AT-GIS implementation. Our prototype is implemented in C++. All geometric operations use the `Boost::Geometry` [17] library, other than the MBR intersection testing, which is hand-written. Aside from the partially-associative JSON parsing, which is done by *RapidJSON* [50], all other transducers are implemented by us. The created AT pipelines for a given query plan are compiled by the GNU g++ compiler. Compilation takes up to 5 seconds, which is negligible compared to the total runtime.

AT-GIS is executed using both fully- and partially-associative transducers to determine the level of optimisation available from reducing speculation: AT-GIS-FAT runs all queries using a fully-associative pipeline with no optimisation; AT-GIS-PAT uses optimised parsers when speculation can be reduced.

System comparisons. We take Hadoop-GIS [1] as an example of a distributed cluster system, which does not use stored indexes beyond the initial partitioning, and SpatialHadoop [13] as an index-based solution. We also compare to PostGIS [25], MonetDB [59] and a commercial DBMS with spatial support (DBMS-X) in terms of single-node spatial query engines. The performance results for SpatialHadoop, PostGIS, MonetDB and DBMS-X results are measured on the same machine as AT-GIS; the results for Hadoop-GIS are based on the same dataset and taken from the paper [1].

For MonetDB, the default set-up has one table with one row per object; in PostGIS, the table is manually sharded into 1000 ranged partitions; and DBMS-X uses a 1024-way spatially partitioned table. The table is indexed by the geometry and clustered by the index prior to query execution.

The experiments are performed using both bounding-box (PostGIS-B, MonetDB-B) and full-geometry comparisons (PostGIS-G,

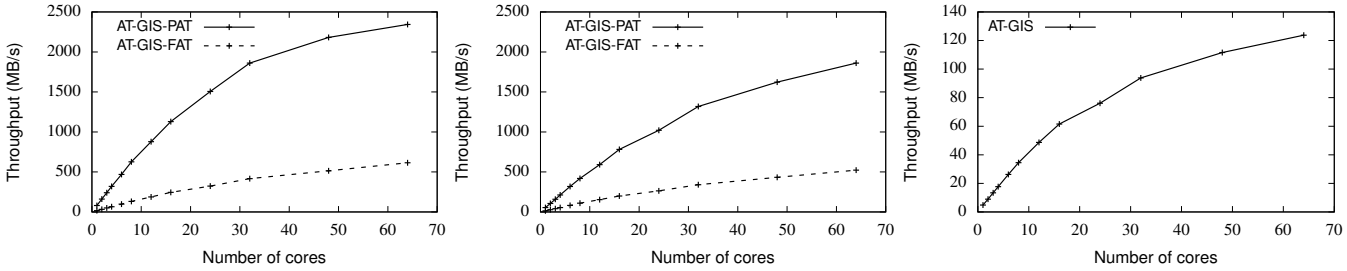

(a) Containment query (b) Aggregation query (c) Join query

Figure 9: Scaling of AT-GIS on the OpenStreetMap dataset

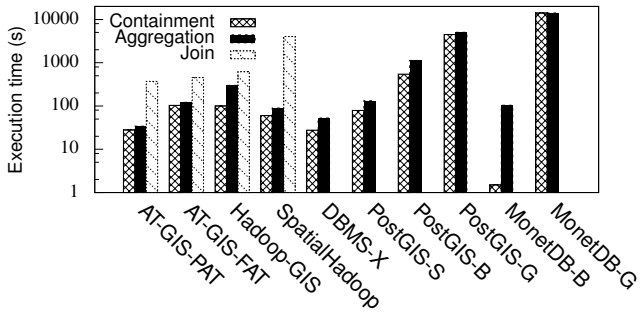

Figure 10: Comparison of query execution times

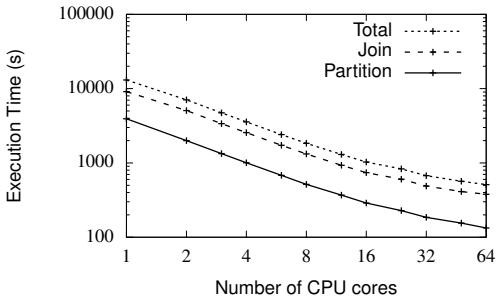

Figure 11: Partition and join query scaling to 64 CPU cores

MonetDB-G). We also manually sharded the PostGIS installation (PostGIS-S). All experiments are repeated and have low variance, which is why we omit error bars.

Experimental set-up. All experiments are performed on a quad-socket, 64-core AMD server with 128 GB RAM. Each CPU has a nominal clock speed of 2.3 GHz, with turbo mode increasing this to 2.9 GHz for small numbers of threads. To limit the effects of I/O bottlenecks, experiments using the OSM-G, OSM-W and Synth datasets read the data from a RAM disk. For experiments using the OSM-10G and OSM-X datasets, we load the data onto an SSD and ensure that the OS file cache is cleared. A second SSD is used to store any temporary data files.

5.1 Query performance

Fig. 10 shows the execution time for three of our queries on different systems.[1] Executing from RAM, AT-GIS-PAT achieves the same query execution time as DBMS-X for the containment query and takes 30% less time for aggregation queries, despite not pre-loading and indexing the data. The results also show the benefit of AT-GIS's efficient pipelining: aggregation takes only 25% longer than containment, outperforming the other comparable systems.

Of all of the RDBMS, MonetDB has the fastest query time for MBR-only queries: using a combination of sequential data access and multithreading, it outperforms the index-based PostGIS and DBMS-X as well as AT-GIS. Once full geometry comparisons are considered, however, the lack of spatial optimisations in MonetDB results in it performing the slowest of all systems.

The results also show that current RDBMS are not optimised for large spatial joins, even with hand-optimised query plans: both PostGIS and DBMS-X do not complete the join within 24 hours, and MonetDB constructs the cross-product of the input prior to joining, requiring over 17 TBs of memory. While executing on a single node, AT-GIS-PAT is 10× faster than SpatialHadoop for the join query due to the latter's cluster management and communication overhead. Hadoop-GIS exhibits the closest join performance to AT-GIS, however, it is deployed on a cluster with more than 3× the number of CPU cores of our server.

For the containment and aggregation queries, the communication overhead of the distributed frameworks becomes even more apparent. Hadoop-GIS requires 3× longer for the aggregation query than for the containment query—the largest disparity of all systems. Taking the number of CPU cores into account, Hadoop-GIS requires 30× the computation resources of AT-GIS-PAT. The upfront indexing of SpatialHadoop improves performance compared to Hadoop-GIS, but it still trails behind AT-GIS on a single node.

The difference between AT-GIS-PAT and AT-GIS-FAT for the containment and aggregation queries shows the dominance of the data parsing cost in terms of the total execution time. Note that the execution times for the other systems do not take the time to load the data into account because this may be amortised over multiple queries. Loading the data can take significant time though, ranging from 30 minutes for MonetDB to over 4 hours for DBMS-X. The data format may also need to be converted prior to loading—no system other than AT-GIS can handle raw OSM XML data.

5.2 Scalability

Next we consider how AT-GIS scales as we vary the number of CPU cores. Figs. 9a and 9b show both full and partial ATs scale to 32 CPU cores for containment and aggregation queries. There are two changes of the gradients in the scaling results: the first occurs after 16 CPU cores and is due to the overclocking of cores with few threads on the AMD CPU; the second change at 32 CPU cores is due to its micro-architecture: the CPU only has 32 FPU units shared between 64 cores. As AT-GIS executes floating-point intensive operations, the scaling beyond 32 cores becomes limited. The contention for FPUs is less of an issue for AT-GIS-FAT because it includes more integer operations when parsing the data.

[1] We do not use the combined query for comparison because the other systems exhibit excessive time or memory requirements when performing the join first.

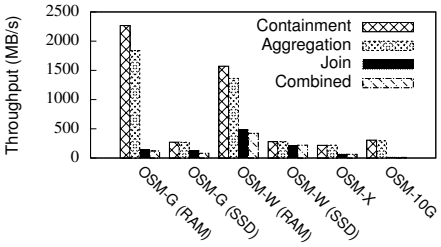

Figure 12: Performance of queries on three data formats

For join queries, Fig. 9c shows that AT-GIS scales linearly to 16 CPU cores followed by two regions (between 16 and 32 cores and greater than 32 cores) when scaling is reduced. The results are only given for AT-GIS-FAT—the parsers used in AT-GIS-PAT do not expose the per-element file offsets required for re-parsing the data in subsequent pipelines.

We explore the join query in more detail in Fig. 11 by splitting the results into the partitioning and the join computation time. It shows that the time required to perform the join dominates the time for the partitioning. The small number of partitions and the high skew between the number of candidate matches checked in each partition makes late finishing threads likely and hard to mitigate. In §5.6, we explore the impact of the number of partitions on the relative performance of the two pipelines used for joining.

5.3 Data size and format

We investigate the ability of AT-GIS to support different input data sizes and formats, in particular, when the dataset is larger than the RAM. We run all four of our queries against each of the OpenStreetMap datasets. As the data sizes on disk vary, and the expected bottleneck is SSD I/O bandwidth, we report throughput in MB/s. Where the dataset is small enough to fit into RAM, we also compare the throughput against streaming from an SSD.

Fig. 12 shows that the GeoJSON format provides superior throughput for single-pass queries because it can use optimised parsers in PAT mode. For join queries, the simpler point structure of WKT allow for faster re-parsing. The SSD results for both GeoJSON and WKT are bound by the device throughput, although OS caching reduces the cost of re-reading data during joins.

OSM-X has the lowest throughput of all single-pass queries due to the large volume of data to be parsed and the need to construct a temporary table. Despite the use of a temporary table, the quantity of data being searched and the random access patterns for finding node values further reduce the performance of joins.

Finally, the replicated dataset (OSM-10G) with single pass-queries executes almost as quickly as the SSD bandwidth allows. It suffers, however, on the join query due to the larger number of comparisons and the need to re-parse data to reduce memory usage.

5.4 Streaming vs. buffered filtering

Next we evaluate the two options for implementing filtering in a pipeline, a *streaming* approach and a *buffered* approach, as described in §4.4. In the streaming approach, the aggregation is performed concurrently with the filter test; in the buffered approach, the geometry is buffered until the result of the filter is known.

We construct a query to output the perimeters of all polygons contained partially or fully by an MBR. By varying the size of the MBR, we can change the query selectivity. The MBR at each size is chosen so that the ratio of MBR size and the number of polygons selected remains constant.

We use two different methods for computing the perimeter to assess how the computational cost affects the trade-off between the two approaches. The first method, shown in Fig. 13a, uses a spherical projection which, while efficient, can be inaccurate for high latitudes. As the ratio of shapes selected becomes less than 25%, the cost of performing the redundant computation becomes greater than that of the memory management for handling the buffers.

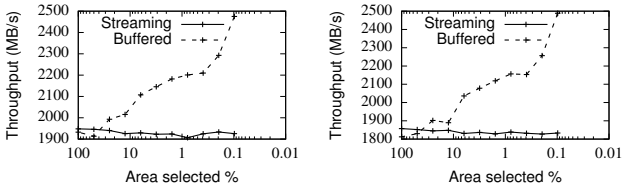

(a) Spherical projection (b) Andoyer's algorithm

Figure 13: Trade-off between different filtering approaches

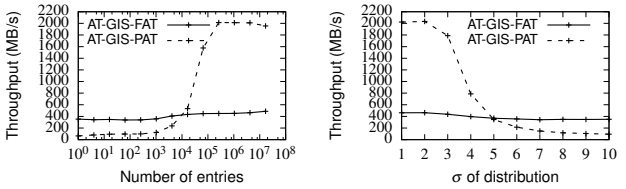

(a) Small numbers of objects (b) Skewed data distribution

Figure 14: Effect of dataset skew

The second method uses Andoyer's algorithm [4], which is more accurate at the expense of more floating-point operations. Fig. 13b shows that the cross-over point between streaming and buffered filtering stays approximately the same, but the absolute throughput of the streaming approach decreases for all selectivities. The buffered approach achieves lower throughput only for low selectivities, which is expected due to the reduced number of calculations when most geometries are rejected by the filter.

5.5 Data skew

In this section, we use a synthetic dataset to explore the limits of partially-associative transducers (AT-GIS-PAT) and the properties of datasets that require fully-associative transducers (AT-GIS-FAT) for parallel operation. We use a synthetic dataset because the objects in the OpenStreetMap dataset are distributed sufficiently, making splitting with partially-associative transducers not a bottleneck. There are two types of datasets that are difficult to split, which we evaluate separately: (i) large datasets consisting of a small number of items; and (ii) datasets with a large skew in polygon complexity.

Fig. 14a shows the processing throughput as we vary the number of objects. For a large number of objects, AT-GIS-PAT can operate around 4× faster than AT-GIS-FAT. This is due to the greater level of optimisation in the off-the-shelf JSON parser and the lack of speculation, leading to less computation. With fewer than 2000 objects, splitting of the dataset becomes the bottleneck in performing the computation—AT-GIS-FAT, which does not need to search for object boundaries, becomes faster.

We also consider the amount of skew in the data distribution. For this, we generate the number of points in each polygon in the synthetic dataset according to a log-normal distribution with a variable σ. For small amounts of skew, the splitting time is negligible, and AT-GIS-PAT performs better, as shown in Fig. 14b. For σ values beyond 5, however, the splitting cost dominates the total processing time, and AT-GIS-FAT provides a lower, more stable processing time.

While AT-GIS-FAT cannot match the speed of the off-the-shelf optimised parser used by AT-GIS-PAT, it performs better with high-skew or low-object-count data. The best of both approaches could be attained by instrumenting the splitting component in partially-associative transducers to fall back to a fully-associative pipeline if the time taken exceeds some threshold.

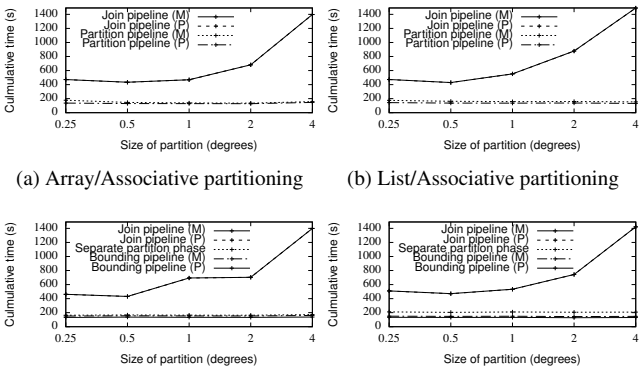

(a) Array/Associative partitioning (b) List/Associative partitioning

(c) Array/Separate partition phase (d) List/Separate partitioning phase

Figure 15: Effect of partition size, storage format and pipeline

5.6 Partitioning and joins

We also investigate (i) whether to run the partitioner as a separate phase or as part of the parsing associative transducer pipeline; (ii) the effect of a varying number of partitions; and (iii) the effect of the data structures used to store the partitions. These experiments are performed on the OpenStreetMap dataset, and the join query finds all intersecting polygons in subsets of the data.

As joining requires two passes, we separately time the Partition pipeline from Fig. 6 and the Join pipeline from Fig. 8. When we perform partitioning as a separate phase, we remove the PARTITION transducer from the Partition pipeline to leave a Bounding pipeline. We measure the time for the processing (P) and merge (M) phases separately for each pipeline.

We first examine the choice between using associative partitioning and a separate partitioning phase. Comparing Figs. 15a and 15c, as the number of partitions increases, there is a small but noticeable increase in the cost of the partition pipeline merge when the partitioner is associative. As would be expected, the merge time is constant when the partitioner is run non-associatively.

Next we consider the size of the partitions (defined in degrees). As can be seen in Figs. 15a–15d, if the partitions are too large, the work becomes unevenly distributed and late-finishing threads cause the total execution time to rise significantly. For small partitions, the cost of partitioning increases, but this is negligible compared to the total query time. The optimum partition size for the dataset is between 0.5 and 1 degrees—there is no further decrease in join time for smaller partitions. Using a partition size of 1 degree could allow for the first pass to employ integer rather than floating-point arithmetic, potentially resulting in a further performance increase.

Finally we consider the choice between linked lists and arrays for storing elements in a partition. Arrays allow for better data locality at the cost of linear-time merging; linked lists require more computation for each element but offer constant-time merging. By comparing Figs. 15a and 15b, we see that the difference does not affect the partitioning time significantly, but the reduced data locality increases the response time by nearly 200 seconds in the worst case. A similar pattern is revealed when comparing Figs. 15c and 15d.

6. RELATED WORK

In addition to the solutions discussed in §2.3, two areas of related work exist to our approach: *parallel automata* have been proposed for structured data parsing [35, 62, 41]; *streaming spatial processing* performs single-pass processing, but it focuses on spatio-temporal queries rather than the bulk data analytics queries as we do.

Parallel automata. The idea behind executing finite automata in parallel is to split the data into blocks and process each block independently. The most common approach, described by Johnson et al. [28] is, for each block, to construct a mapping between all possible starting states and the corresponding finishing states. Once constructed, these mappings can be combined to compute the final state. Johnson et al. have the goal to save memory when processing streams of network traffic, with packets arriving out-of-order, but they do not optimise performance.

More recently, *simultaneous finite automata* (SFA) [56] perform a static construction to improve performance at the expense of a potentially expensive compilation. The result is near-linear scaling, albeit on a limited set of benchmarks. We use ideas from both Johnson and SFA and extend them to emit symbols for the next stage in a pipeline. In particular, for all the data formats that we consider, the first stage in any pipeline is a lexer, which can be described by a deterministic finite transducer. We also reduce the size of the constructed automaton using format-specific knowledge.

There have also been other approaches to parallel lexing and parsing of structured documents [35]. Early techniques used a sequential data pre-scan to determine suitable break points; this was enhanced by exploiting special strings to guess the correct lexer state [62]. This mirrors our approach for partially associative transducers, which reduce the state space based on knowledge of the input format. Our approach goes further and can use markers in the data to specify the initial state of multiple stages in the pipeline.

Parallel pushdown transducers [41] extend parallel automata to pushdown transducers used in XML querying, with near-linear scaling for a small number of queries. The work does not explore composition, relying on sequential post-processing to perform filtering. Using composition, we present a more powerful model for parallel computation that goes beyond structural queries.

Streaming spatial query processing. There is an increasing interest in using stream processing with spatial datasets, especially with the growth of sensor networks [5, 52] and IoT use cases [11]. For example, *StreamInsight* [29] has spatial primitives to support spatial predicates over complex streams. Isenburg et al. [27] describe a number of streaming algorithms for 3D modelling and use windows to handle models that are larger than memory.

While streaming systems can answer temporal streaming queries, they are not designed for joins across an entire dataset as this is counter to their processing model over unbounded streams. In addition, single-node streaming engines typically focus on query- and not data-parallelism [20, 14]. By processing finite datasets with high parallelism, we designed a more flexible spatial engine without the windowing support of streaming systems. ATs do not presently have an efficient primitive for sliding windows [30].

7. CONCLUSION

We have described AT-GIS, a new single-node system for parallel spatial query processing that is capable of exploiting previously unavailable data parallelism using *associative transducers* (ATs). AT-GIS operates on input formats directly, avoiding expensive conversions, and thus significantly reduces data-to-query time.

AT-GIS shows good scaling behaviour for single-pass spatial queries on un-indexed data, even matching the performance of index-based systems for simple queries. Given the lack of pre-built indices, it can order filtering operations to minimise the cost of joins, while maintaining parallelism through partitioning. However, compared to large cluster-based systems, AT-GIS exhibits worse performance for large joins (>200 million elements) due to its simple partitioning scheme and the limits of single-node computation.

We have focussed on situations in which there is no knowledge of past data. Based on our experience with the XML-formatted data, our future works plans to explore how *incremental* changes in large datasets can be handled efficiently through the storage of intermediate results and lightweight index construction.

8. REFERENCES

[1] A. Aji, F. Wang, H. Vo, R. Lee, Q. Liu, X. Zhang, and J. Saltz. Hadoop-GIS: A high performance spatial data warehousing system over mapreduce. *Proc. VLDB Endow.*, 6(11), 2013.

[2] I. Alagiannis, R. Borovica, M. Branco, S. Idreos, and A. Ailamaki. NoDB: Efficient query execution on raw data files. In *SIGMOD*, 2012.

[3] J. C. Anderson, J. Lehnardt, and N. Slater. *CouchDB: The definitive guide*. O'Reilly, 2010.

[4] H. Andoyer. *Cours D'Astronomie*. 1909.

[5] M. Batty. Big data, smart cities and city planning. *Dialogues in Human Geography*, 3(3), 2013.

[6] P. A. Boncz, M. Zukowski, and N. Nes. MonetDB/X100: Hyper-pipelining query execution. In *CIDR*, volume 5, 2005.

[7] M. Botts, G. Percivall, C. Reed, and J. Davidson. OGC sensor web enablement: Overview and high level architecture. In *GeoSensor networks*. 2008.

[8] T. Bray. The JavaScript Object Notation (JSON) Data Interchange Format. RFC 7159, 2014.

[9] J. R. Davis. IBM's DB2 spatial extender: Managing geo-spatial information within the DBMS. *IBM Corporation*, 1998.

[10] J. Dean and S. Ghemawat. MapReduce: Simplified data processing on large clusters. *Communications of the ACM*, 51(1), 2008.

[11] DEBS Grand Challenge. http://www.debs2015.org/call-grand-challenge.html, 2015.

[12] M. J. Egenhofer. Toward the semantic geospatial web. In *SIGSPATIAL*. ACM, 2002.

[13] A. Eldawy and M. F. Mokbel. SpatialHadoop: A MapReduce framework for spatial data. In *ICDE*, 2015.

[14] Esper Stream Processing Engine. http://www.espertech.com/esper, 2015.

[15] Y. Fang, M. Friedman, G. Nair, M. Rys, and A.-E. Schmid. Spatial indexing in Microsoft SQL Server 2008. In *SIGMOD*, 2008.

[16] G. Garbis, K. Kyzirakos, and M. Koubarakis. Geographica: A benchmark for geospatial RDF stores. In *ISWC*. 2013.

[17] B. Gehrels, B. Lalande, M. Loskot, and A. Wulkiewicz. Boost geometry library, 2014.

[18] GeoCouch. http://github.com/couchbase/geocouch, 2015.

[19] GeoJSON specification. http://geojson.org/geojson-spec.html, 2015.

[20] V. Gulisano, R. Jimenez-Peris, M. Patino-Martinez, C. Soriente, and P. Valduriez. Streamcloud: An elastic and scalable data streaming system. *IEEE TPDS*, 23(12), 2012.

[21] M. Haklay and P. Weber. OpenStreetMap: User-generated street maps. *IEEE Pervasive Computing*, 7(4), 2008.

[22] S. E. Hampton, C. A. Strasser, J. J. Tewksbury, W. K. Gram, A. E. Budden, A. L. Batcheller, C. S. Duke, and J. H. Porter. Big data and the future of ecology. *Frontiers in Ecology and the Environment*, 11(3), 2013.

[23] S. I. Hay, D. B. George, C. L. Moyes, and J. S. Brownstein. Big data opportunities for global infectious disease surveillance. *PLoS Med*, 10(4), 2013.

[24] E. G. Hoel and H. Samet. Data-parallel spatial join algorithms. In *ICPP*, 1994.

[25] S. Holl and H. Plum. PostGIS. *GeoInformatics*, 3(2009), 2009.

[26] M. Isard and Y. Yu. Distributed data-parallel computing using a high-level programming language. In *SIGMOD*, 2009.

[27] M. Isenburg and P. Lindstrom. Streaming meshes. In *IEEE Visualization*, 2005.

[28] T. Johnson, S. Muthukrishnan, and I. Rozenbaum. Monitoring regular expressions on out-of-order streams. In *ICDE*, 2007.

[29] S. J. Kazemitabar, U. Demiryurek, M. Ali, A. Akdogan, and C. Shahabi. Geospatial stream query processing using Microsoft SQL Server StreamInsight. *Proc. VLDB Endow.*, 3(1-2), 2010.

[30] A. Koliousis, M. Weidlich, R. C. Fernandez, A. Wolf, P. Costa, and P. Pietzuch. SABER: Window-based hybrid stream processing for heterogeneous architectures. In *SIGMOD*, 2016.

[31] J. Kong, L. A. Cooper, F. Wang, D. Gutman, J. Gao, C. Chisolm, A. Sharma, T. Pan, E. G. Van Meir, T. M. Kurc, et al. Integrative, multimodal analysis of glioblastoma using TCGA molecular data, pathology images, and clinical outcomes. *IEEE Trans. on Biomedical Engineering*, 58(12), 2011.

[32] R. K. V. Kothuri, S. Ravada, and D. Abugov. Quadtree and R-tree indexes in Oracle Spatial: A comparison using GIS data. In *SIGMOD*, 2002.

[33] J.-G. Lee and M. Kang. Geospatial big data: Challenges and opportunities. *Big Data Research*, 2(2), 2015.

[34] X. Liu, J. Han, et al. Implementing WebGIS on Hadoop: A case study of improving small file I/O performance on HDFS. In *CLUSTER*, 2009.

[35] W. Lu, K. Chiu, and Y. Pan. A parallel approach to XML parsing. In *Grid Computing*, 2006.

[36] A. Meduna. Finite and pushdown transducers. In *Automata and Languages*. 2000.

[37] V. Mische. GeoCouch: A spatial index for CouchDB. *Presentation at FOSS4G*, 2010.

[38] MonetDB GeoSpatial. https://www.monetdb.org/Documentation/Extensions/GIS, 2015.

[39] MySQL 5.0 Reference Manual (11.5. Extensions for Spatial Data). https://dev.mysql.com/doc/refman/5.0/en/, 2015.

[40] T. T. Nguyen. Indexing PostGIS databases and spatial query performance evaluations. *International Journal of Geoinformatics*, 5(3), 2009.

[41] P. Ogden, D. Thomas, and P. Pietzuch. Scalable XML query processing using parallel pushdown transducers. *Proc. VLDB Endow.*, 6(14), 2013.

[42] Open Geospatial Consortium, Simple feature access specification. http://www.opengeospatial.org/standards/sfa, 2015.

[43] OpenDStreetMap XML format. http://wiki.openstreetmap.org/wiki/OSM_XML, 2015.

[44] OpenStreetMap mirror, 2015/05/18. ftp://ftp.spline.de/pub/openstreetmap/planet/2015/planet-150518.osm.bz2, 2015.

[45] Oracle Corporation. Oracle Spatial and Graph: Advanced data management. 2014.

[46] Y. Pan, Y. Zhang, and K. Chiu. Simultaneous transducers for data-parallel XML parsing. In *IPDPS*, 2008.

[47] A. Papadopoulos and Y. Manolopoulos. Parallel bulk-loading of spatial data. *Parallel Computing*, 29(10), 2003.

[48] J. M. Patel and D. J. DeWitt. Partition-based spatial-merge join. In *SIGMOD*, volume 25, 1996.

[49] F. Peng and S. S. Chawathe. XPath queries on streaming data. In *SIGMOD*, 2003.

[50] RapidJSON. https://github.com/miloyip/rapidjson, 2015.

[51] S. Ray, B. Simion, and A. Demke Brown. Jackpine: A benchmark to evaluate spatial database performance. In

ICDE, 2011.

[52] S. Shekhar, V. Gunturi, M. R. Evans, and K. Yang. Spatial big-data challenges intersecting mobility and cloud computing. In *MobiDE*, 2012.

[53] A. Silberschatz, H. Korth, and S. Sudarshan. *Database systems concepts*. McGraw-Hill, Inc., 6 edition, 2010.

[54] B. Simion, D. N. Ilha, A. D. Brown, and R. Johnson. The price of generality in spatial indexing. In *BigSpatial*, 2013.

[55] Simple API for XML. http://sax.sourceforge.net/, 2015.

[56] R. Sinya, K. Matsuzaki, and M. Sassa. Simultaneous finite automata: An efficient data-parallel model for regular expression matching. In *ICPP*, 2013.

[57] H. Sutter. The free lunch is over: A fundamental turn toward concurrency in software. *Dr. Dobb's journal*, 30(3), 2005.

[58] O. Tange et al. Gnu parallel: The command-line power tool. *The USENIX Magazine*, 36(1), 2011.

[59] M. Vermeij, W. Quak, M. Kersten, and N. Nes. MonetDB: A novel spatial column store DBMS. In *FOSS4G*, 2008.

[60] F. Wang, J. Kong, L. Cooper, T. Pan, T. Kurc, W. Chen, A. Sharma, C. Niedermayr, T. Oh, D. Brat, A. Farris, D. Foran, and J. Saltz. A data model and database for high-resolution pathology analytical image informatics. *Journal of Pathology Informatics*, 2(1), 2011.

[61] L. Xiao and Z. Wang. Internet of things: A new application for intelligent traffic monitoring system. *Journal of networks*, 6(6), 2011.

[62] C.-H. You and S.-D. Wang. A data parallel approach to XML parsing and query. In *HPCC*, 2011.

[63] Q. Zhou and J. Zhang. Research prospect of Internet of Things geography. In *Geoinformatics*, 2011.